Proceedings of the ASME 2020
Internal Combustion Engine Division Fall Technical Conference
ICEF2020
November 1-4, 2020, Denver, CO, USA

ICEF2020-2929

GASOLINE COMPRESSION IGNITION (GCI) ON A LIGHT-DUTY MULTI-CYLINDER ENGINE USING A WIDE RANGE OF FUEL REACTIVITIES & HEAVY FUEL STRATIFICATION[1]

Adam B. Dempsey
Marquette University
Milwaukee, WI, USA

Scott Curran & Robert Wagner
Oak Ridge National Laboratory
Oak Ridge, TN, USA

William Cannella
Chevron Energy Technology Company
Richmond, CA, USA

Andrew Ickes
Chevron Energy Technology Company
Richmond, CA, USA

ABSTRACT

Many research studies have focused on utilizing gasoline in modern compression ignition engines to reduce emissions and improve efficiency. Collectively, this combustion mode has become known as gasoline compression ignition (GCI). One of the biggest challenges with GCI operation is maintaining control over the combustion process through the fuel injection strategy, such that the engine can be controlled on a cycle-by-cycle basis. Research studies have investigated a wide variety of GCI injection strategies (i.e., fuel stratification levels) to maintain control over the heat release rate while achieving low temperature combustion (LTC). This work shows that at loads relevant to light-duty engines, partial fuel stratification (PFS) with gasoline provides very little controllability over the timing of combustion. On the contrary, heavy fuel stratification (HFS) provides very linear and pronounced control over the timing of combustion. However, the HFS strategy has challenges achieving LTC operation due to the air handling burdens associated with the high EGR rates that are required to reduce NOx emissions to near zero levels. In this work, a wide variety of gasoline fuel reactivities (octane numbers ranging from <40 to 87) were investigated to understand the engine performance and emissions of HFS-GCI operation on a multi-cylinder light-duty engine. The results indicate that over an EGR sweep at 4 bar BMEP, the gasoline fuels can achieve LTC operation with ultra-low NOx and soot emissions, while conventional diesel combustion (CDC) is unable to simultaneously achieve low NOx and soot. At 10 bar BMEP, all the gasoline fuels were compared to diesel, but using mixing controlled combustion and not LTC.

INTRODUCTION

Low temperature combustion (LTC) in compression ignition engines can yield ultra-low NOx and soot emissions while maintaining high thermal efficiency. To achieve LTC, sufficient mixing time between the fuel and air in a globally dilute environment is required, thereby avoiding fuel rich regions and reducing peak combustion temperatures, which significantly reduces soot and NOx formation, respectively. Gasoline has a higher volatility and lower chemical reactivity compared to diesel fuel, meaning it is easier to achieve the amount of premixing time required prior to autoignition to achieve LTC. Therefore, many recent research studies have focused on utilizing gasoline as an enabler for LTC operation in compression ignition engines.

However, regardless of the fuel, one of the biggest challenges with LTC operation is maintaining control over the combustion process through the fuel injection strategy, such that the engine can be controlled on a cycle-by-cycle basis. Previous work by the authors highlighted the spectrum of fuel stratification strategies for gasoline compression ignition (GCI) engines from partial to heavy fuel stratification [1]. Figure 1 shows examples of common fuel injection strategies to achieve partial (PFS), moderate (MFS), and heavy (HFS) fuel stratification with GCI. The injection strategies shown here are somewhat arbitrary but are guided by common themes in the literature. PFS can use port fuel injection or very early direct injection during the intake stroke to create a homogeneous charge of fuel and air. Subsequent direct injections occur during the compression stroke to create slight levels of fuel stratification in an attempt to create sequential autoignition events while maintaining ultra-low NOx and soot emissions [2]–[7]. MFS increases the stratification level by reducing to the amount of premixed fuel and typically features all direct injections during the compression stroke. In addition, MFS strategies typically feature a fuel injection event near top dead center (TDC) of the compression stroke to trigger combustion [8]–[12]. Lastly, HFS utilizes the highest level of fuel stratification and typically features no premixed fuel and direct injection(s) relatively close to TDC [13]–[19]. HFS tends to utilize higher fuel injection pressure compared to PFS and MFS, as illustrated in Figure 1 by the bar height.

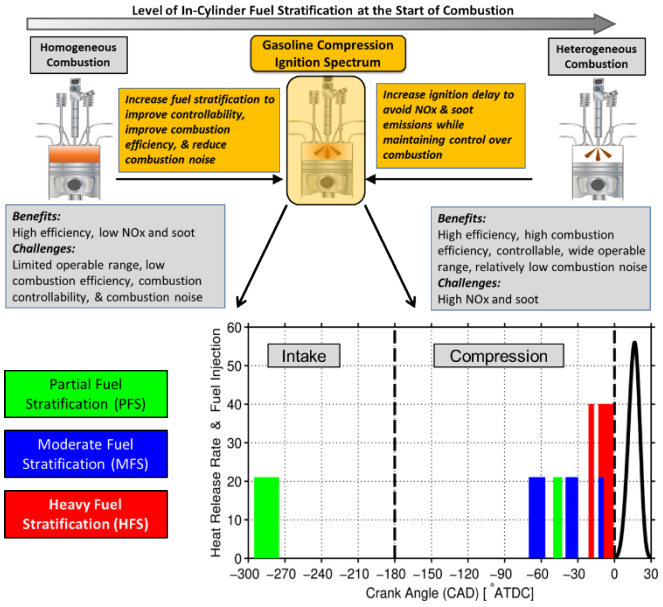

Figure 1: Range of in-cylinder fuel stratification for compression ignition engines. This manuscript focuses on GCI operation with PFS and HFS injection strategies.

A mechanism for controlling the combustion process is required for any advanced combustion strategy to be implemented in a production intent application. In this work, it will be shown that at loads relevant to light-duty engines, PFS with gasoline provides very little controllability over the timing of combustion. On the contrary, HFS provides very linear and pronounced control over the timing of combustion. Therefore, this study will focus on HFS operation due to its superior combustion control authority. However, HFS operation has challenges achieving LTC operation due to the air handling burdens associated with high EGR rates.

Combustion strategy development is typically conducted using single-cylinder engines due to their highly flexible air system and ability to control boundary pressures, air flow, and EGR flow independent of the limitations of turbomachinery. As much as these studies are a necessary first step to designing an LTC operating strategy that maximizes indicated efficiency, it is important to realize that on a production multi-cylinder engine,

the intake pressure and EGR rate typically cannot be varied independently to a great extent. Therefore, this work will use a production, light-duty multi-cylinder engine to study HFS-GCI operation with a variety of gasoline fuel reactivities and build an understanding of which fuels are able to achieve LTC operation.

These experiments focused on using gasolines that have octane numbers lower than market gasoline. Low octane gasoline fuels for compression ignition engines are attractive for a variety of reasons. From a fuel production standpoint, some lower octane streams are present in refineries, but are usually upgraded to produce higher octane market gasolines. The use of lower octane gasolines could require less refinery octane upgrading and thus, in theory, produce less CO_2 emissions during production [20]. From an engine combustion standpoint, the lower octane gasoline fuels have been shown to cover a wider operating range for GCI operation while yielding lower combustion noise than conventional, higher octane gasolines [21]. Finally, for more premixed strategies, the ignition delay of low octane gasolines has been shown to be sensitive to the mixture equivalence ratio, thus allowing fuel stratification to be a potential method to control the timing and rate of heat release [22].

This work, through experiments with a wide range of custom fuels and coupled multi-dimensional Computational Fluid Dynamic (CFD) simulations, aims to provide additional understanding of the role of gasoline octane number to achieve LTC operation with GCI in a production light-duty compression ignition engine. The results of this research demonstrate that at mid-load conditions, relevant to light-duty engines, PFS operation can yield high efficiency and low emissions. However, PFS was unable to provide adequate levels of combustion timing controllability. Therefore, the focus was shifted to HFS operation, for which it was shown that the timing of combustion is readily controllable, much like conventional diesel combustion. Lastly, using HFS operation, a wide variety of fuel reactivities were investigated. At mid-load conditions, it was shown that all the gasoline like fuels reduce soot emissions relative to diesel fuel, but the higher octane gasoline fuels have relatively low EGR tolerance due to overmixing. At a higher load condition, all the gasoline fuels tend to converge in the behavior and the effects of fuel reactivity are diminished.

EXPERIMENTAL ENGINE & LABORATORY SETUP

The engine used for this study was a modified 2007 GM direct injection 1.9 L diesel engine. The base engine geometric specifications are shown in Table 1. The engine is equipped with four variable swirl actuators (VSA): one for each cylinder. The swirl ratio is controlled by throttling one of the intake ports for each cylinder while the other port is completely unthrottled. When the throttled port is fully open, the swirl ratio is at its minimum of ~2.0. By fully closing the throttle, the swirl ratio can be increased to ~5.0, but this has been shown to significantly increase the pumping parasitic [7]. The original equipment manufacturer (OEM) pistons, common rail direct injection (DI) system, and variable geometry turbocharger (VGT) were left in production form. An aftermarket charge air cooler (CAC) was installed. Figure 2 shows the overall engine and fuel system layout.

The stock engine control unit was replaced with a full-pass control system from National Instruments - Powertrain Controls Group (formerly Drivven, Inc.), which allowed simultaneous control of each DI injector, allowing for cylinder-to-cylinder balancing as well as all other relevant engine parameters, such as rail pressure, VGT position, and VSA position.

Table 1: Geometric specifications of a model year 2007 GM 1.9 L compression ignition engine

Number of cylinders	4
Bore [mm]	82.0
Stroke [mm]	90.4
Connecting rod length [mm]	145.4
Compression Ratio [-]	16.5
Total displacement [L]	1.9
Intake valve open (IVO)* [°ATDC]	344°
Intake valve close (IVC)* [°ATDC]	-132°
Exhaust valve open (EVO)* [°ATDC]	116°
Exhaust valve close (EVC)* [°ATDC]	-340°

*Valve timings taken at 0.1 mm valve lift.

The production Bosch CRI2.2 injector is a high pressure, solenoid-driven, common rail fuel injector that was mounted vertically and in the center of each cylinder. The production 7-hole, mini-sac injector tip was used, which has an included angle of 148° (16° down-angle from the fire deck, i.e., the bottom surface of the cylinder head) and a nominal hole diameter of 140 μm.

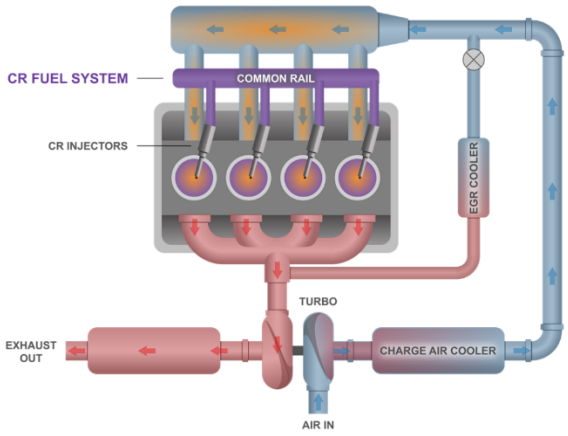

Figure 2: Multi-cylinder GM 1.9 L engine schematic. The DI injectors are shown on an angle for illustrative purposes but are mounted vertically in the cylinder head.

Figure 3 illustrates the DI combustion system showing the piston bowl shape and the spray targeting of the 148° included angle injectors. The piston bowl is relatively deep and narrow

with a re-entrant shape. This is a conventional light-duty diesel piston shape from this vintage diesel engine. It is shown that with injection timings earlier than approximately -25° ATDC, the DI fuel has the potential to miss the bowl and be injected into the squish region.

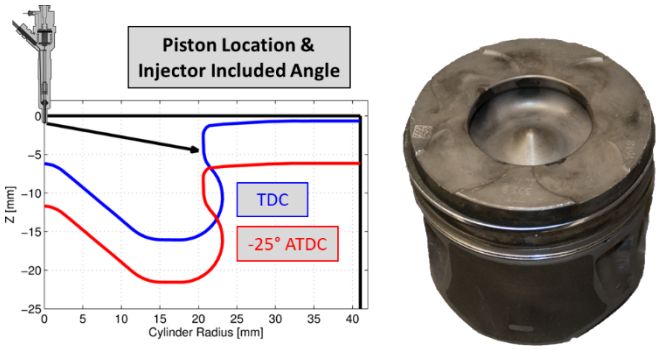

Figure 3: a) Illustration of direct injected combustion system at two different crank angle locations and b) photograph of the OEM light-duty piston.

The DI fuel system was left in the stock form except that the polymer injector return lines were replaced with stainless steel leading to the stock damper. Since the DI fuel system was not designed for high volatility fuels, extra care was taken to prevent fuel vapor from forming in the system or potential cavitation before the fuel meter or high pressure Bosch CP1H pump. A Max Machinery 710 Fuel Measurement system was used to supply fuel to the high pressure fuel pump at ~4.15 bar. The fuel system consists of a fuel conditioning and measurement package. The fuel conditioner contains a vapor eliminator along with regulators, internal heat exchangers, level controller, and lift pump. A positive displacement volumetric flow measurement system, which was used to record the instantaneous fuel flow to the engine. Heat exchangers were added to the supply and return lines, which were cooled using an external chiller set to 15°C. A schematic of the fuel system is shown in Figure 4.

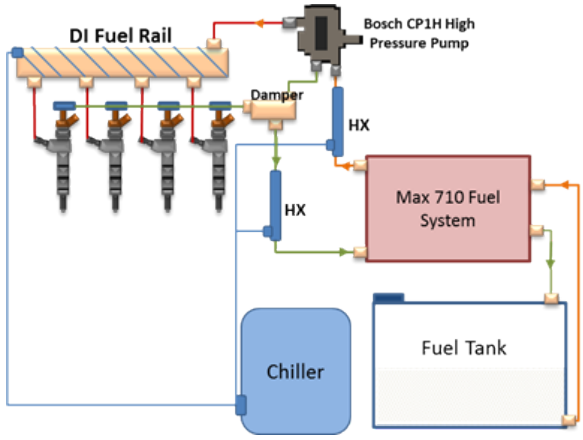

Figure 4: Fuel system configuration for measurement and conditioning for high pressure direct injection of gasoline.

The brake torque produced by the engine was measured using T40B inline torque transducer made by HBM, Inc. The intake fresh air flow rate was measured using a laminar flow element. Conditioned air was supplied to the engine's turbocharger compressor inlet at a constant temperature of 25°C and a relative humidity of 60%. The engine coolant and oil temperature were maintained at 90°C. High-speed in-cylinder pressure data were acquired using Kistler model 6058A pressure transducers installed in the glow plug ports of all four cylinders. Individual Kistler type 5010 dual-mode amplifiers were used to process the pressure signals and the built-in combustion package from National Instruments/Drivven was used to process the data. Combustion metrics were monitored and recorded using the Drivven combustion analysis toolkit (DCAT). Cylinder pressure was pegged to the intake manifold pressure bottom dead center (BDC) of the intake stroke and sampled at a resolution of 0.2 crank angle degrees. High-speed data (i.e., in-cylinder pressure) was recorded for 300 consecutive engine cycles. The low-speed data (air flow, fuel flow, boundary conditions, and emissions) were recorded for 180 seconds at ~2 Hz.

In a multi-cylinder engine, there are variations in conditions from cylinder to cylinder, such as wall temperature, EGR level, trapped residuals, total fuel delivered, etc. Kinetically controlled combustion strategies are especially sensitive to changes in these types of parameters. This can lead to significant cylinder to cylinder imbalances in the combustion phasing (CA50), indicated mean effective pressure (IMEP), peak pressure rise rate (PPRR), and emissions. To adjust for these variations and maintain a nearly constant combustion phasing and load from each cylinder, this engine controller was setup to vary the total fueling and start of injection commands (SOIc) independently for each cylinder. This will be important in this work and will be highlighted in a subsequent section.

Exhaust emissions were measured using standard gaseous emissions analyzers. A heated flame ionization detector was used to measure total unburned hydrocarbons (UHC). The UHC emissions are reported on a C1-basis. A heated chemiluminescence analyzer was used to measure total NOx emissions ($NO + NO_2$). Both CO and CO_2 were measured using

non-dispersive infrared (NDIR) instruments. Intake and exhaust O_2 were measured using a paramagnetic detector (PMD). The exhaust sample stream was conveyed from heated filters to the instruments through heated lines maintained at 190°C. An AVL 415S smoke meter was used to measure the filter smoke number (FSN), which is an indicator of black carbon containing soot in the exhaust.

EXPERIMENTAL DATA ANALYSIS

At each operating condition, the 300 consecutive cycles of cylinder pressure data collected were ensemble averaged to yield a representative cylinder pressure trace for each cylinder, which was used to calculate the average apparent heat release rate (AHRR) for each cylinder. The AHRR is determined from a first law of thermodynamics balance on the cylinder contents. It is essentially the chemical heat release rate minus the heat loss rate to the combustion chamber walls, and is given by

$$AHRR = \left.\frac{dQ}{d\Theta}\right|_{chem} - \left.\frac{dQ}{d\Theta}\right|_{wall} = \frac{1}{\gamma - 1} V \frac{dP}{d\Theta} + \frac{\gamma}{\gamma - 1} P \frac{dV}{d\Theta} \quad (1)$$

where P is the average in-cylinder pressure, V is the cylinder volume, and γ is the ratio of specific heats for the in-cylinder gas mixture. In this work, the average cylinder pressure and AHRR traces will be shown from cylinder #2.

The indicated cycle work is given by

$$W_{cycle} = \oint_{cycle} P dV \quad (2)$$

where the gross cycle is comprised of the compression and expansion strokes only (-180° to 180° ATDC, where 0° ATDC represents top dead center of the compression stroke). The net cycle is made up of the entire four-stroke cycle (-360° to 360° ATDC). Lastly, the pumping cycle consists of the exhaust and intake strokes (180° to -180° ATDC), which is the difference between the net and gross cycles. The cycle indicated efficiencies are calculated as

$$IE_{cycle} = \frac{\sum_{i=1}^{N_{cyl}=4} W_{cycle,cyl_i}}{m_{fuel} LHV_{fuel}} \quad (3)$$

where the cycle work ($W_{cycle,cyl,i}$) is summed across all 4 cylinders of the engine, the fuel mass (m_{fuel}) is taken as the total fuel delivered to the engine, and LHV_{fuel} is the lower heating value of the fuel. It is important that the gross and net cycle indicated efficiencies are calculated this way rather than isolating a single cylinder because the fueling to each individual cylinder is unknown and assuming that the fueling to each cylinder is equal is not an appropriate assumption.

The measured exhaust emissions are processed, correcting for dry-to-wet conversions (where applicable) and computing the true exhaust mole fractions of each species of interest. The true exhaust mole fractions (x_i) can be used in a variety of calculations. The combustion efficiency is calculated as

$$\eta_{comb} = \frac{1 - n_{exh}\left[x_{CO} MW_{CO} LHV_{CO} + x_{HC} MW_{fuel} LHV_{fuel}\right]}{LHV_{fuel} MW_{fuel}} \quad (4)$$

where n_{exh} is the number of moles of exhaust per mole of fuel, x_i is the mole fraction of exhaust species i, and MW is the molecular weight. In this work, brake specific (BS) emissions are presented, which are calculated as

$$BS_i = \frac{n_{exh} x_i MW_i \dot{m}_{fuel}}{BP * MW_{fuel}} \left[\frac{g_i}{kW - hr}\right] \quad (5)$$

where BP is the engine brake power computed from measured brake torque and engine speed.

The external cooled EGR level is calculated as

$$EGR\ [\%] = 100 * \frac{x_{CO_2,int} - x_{CO_2,air}}{x_{CO_2,exh} - x_{CO_2,air}} \quad (6)$$

where $x_{CO_2,int}$ is the intake CO_2 mole fraction, $x_{CO_2,exh}$ is the exhaust CO_2 mole fraction, and $x_{CO_2,air}$ is the ambient CO_2 mole fraction.

The true exhaust mole fractions, fuel flowmeter, and air flowmeter were used to calculate three independent air/fuel ratios, as outlined in reference [23]. The aim is for these air/fuel ratios to agree, which ensures data quality and provides a check of the accuracy of the individual measurement devices. In this work, the three air/fuel ratios agreed to within 4% for all the data points recorded.

IN-CYLINDER CFD SIMULATIONS

Multi-dimensional CFD simulations were used in conjunction with the engine experiments to provide insight into some of the experimental observations. The KIVA3V Release 2 CFD code was used [24]–[26]. The model uses the most popular approach for modeling engine sprays, the Lagrangian-Drop Eulerian-Fluid (LDEF) method, in which liquid fuel is treated as Lagrangian parcels and the ambient gas is discretized into Eulerian cells. Figure 5 shows a high-level illustration of the CFD modeling approach and the physical and chemical processes considered [1].

The combustion model uses a well-stirred reactor assumption, treating each CFD cell as homogeneous, and conducts semi-detailed chemical kinetic calculations in each cell at each timestep to calculate the rate of change of all gas phase species. The gas phase kinetic mechanism was developed by Ra and Reitz for PRF fuels and consists of 47 species and 142 elementary reactions [27].

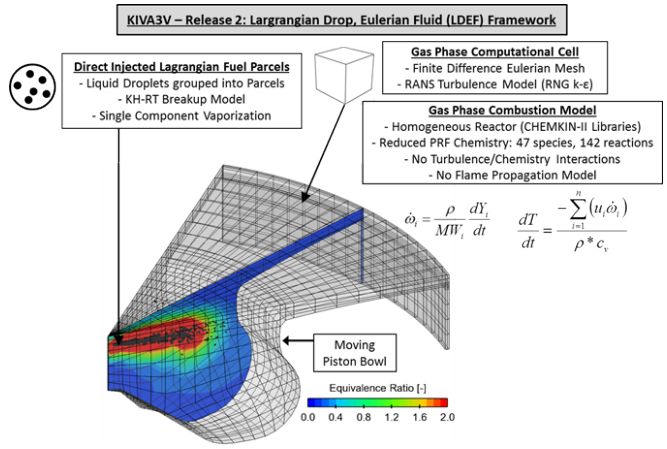

Figure 5: Illustrative overview of the CFD modeling approach for in-cylinder engine processes (e.g., liquid fuel injection, spray breakup, droplet evaporation, turbulent mixing, and combustion).

Several sub-model improvements have been made to the KIVA3V code at the University of Wisconsin-Madison's Engine Research Center, including fuel droplet breakup, droplet evaporation, droplet collision modeling, turbulence modeling, and semi-detailed chemical kinetics. For the sake of brevity these sub-model improvements will not be discussed here. For a brief overview of the simulation methodology and sub-model improvements, see Dempsey et al. [23], [28]. For a detailed review of the CFD modeling approach, see the lecture series given by Professor Rolf Reitz [29].

FUELS

In this study, a wide variety of fuels were investigated. The relevant fuel properties are shown in Table 2. A conventional ultra-low sulfur diesel (ULSD) fuel was used along with a variety of gasoline boiling range fuels (hereafter referred to as gasoline fuels). All the gasoline fuels had gasoline-like volatility, but a wide range of fuel reactivity (i.e., octane number). As shown in the table, the gasoline reactivities range from diesel-like, with octane numbers less than 40, all the way to a research octane number (RON) of 87, which is slightly more reactive than a market regular grade gasoline in the United States. Therefore, the range of gasoline fuels used in this study would be classified as low octane gasolines, relative to commercially available gasolines.

As shown in the table, some of the gasoline fuels contain reactivity enhancing additives to reduce their octane number. These additives are 2-ethyl hexyl nitrate (EHN) and di-tert butyl peroxide (DTBP). These additives and their impact on gasoline reactivity have been studied previously by the authors [30], [31] and will be elaborated on in this study. All of the gasoline fuels were additized with a lubricity additive, with a concentration of ~500 ppm, to protect the high pressure fuel pump and injectors.

Table 2: Fuel properties for the diesel fuel and various gasoline fuels investigated. The line above each fuel is a legend indicating the line style and color that will be used in all subsequent plots. An asterisk (*) next to the fuel name signifies that it contains EHN.

		Gasoline Fuels						
	Diesel	<40RON*	<40RON	68RON	72RON*	72RON	75RON	87RON
RON	-	<40	<40	68	72.4	72	75.9	87.1
MON	-	<40	<40	66	73.3	73.6	73.2	81.3
Cetane	45.3	-	-	26	24.2	24.3	22.7	18
Density [g/cc]	0.849	0.718	0.715	0.706	0.714	0.713	0.709	0.712
LHV [MJ/kg]	42.63	43.65	43.76	44.38	44.15	43.95	44.32	44.15
C [wt%]	86.9%	84.3%	84.4%	84.8%	84.9%	84.9%	84.9%	85.0%
H [wt%]	13.1%	14.8%	14.9%	15.2%	14.9%	15.0%	15.1%	15.0%
O [wt%]	0%	0.69%	0.74%	0%	0.14%	0.16%	0%	0%
N [wt%]	0%	0.2%	0%	0%	0.04%	0%	0%	0%
EHN [vol%]	-	2.5%	-	-	0.5%	-	-	-
DTBP [vol%]	-	-	3.4%	-	-	0.75%	-	-

COMBUSTION TIMING CONTROLLABILITY: PARTIAL FUEL STRATIFICATION (PFS) VS. HEAVY FUEL STRATIFCATION (HFS)

For any advanced engine combustion strategy to be adopted into the transportation marketplace, it must have a mechanism by which to control the timing of combustion. This is necessary for the engine to have a wide operable speed/load space, respond to changes in the environmental conditions and fuel properties, and allow for rapid transient response. The authors have previously studied two forms of GCI: partial fuel stratification (PFS) [1], [7] and heavy fuel stratification (HFS) [1]. Both combustion modes show promise to reduce the NOx and soot emissions from diesel engines, but there is an open question as to which provides an adequate level of combustion timing controllability on a light-duty multi-cylinder engine at operating conditions representative of light-duty driving.

Using the 68 RON gasoline fuel PFS and HFS operation were compared to understand the level of combustion timing control authority each strategy can deliver. The comparison was conducted at an engine speed of 2000 rpm and an engine load of 4 bar brake mean effective pressure (BMEP), which is a representative light-duty driving condition, as stated by the USCAR Advanced Combustion & Emissions Control (ACEC) tech team [32].

As illustrated in Figure 1, the PFS strategy used a double direct injection with a rail pressure of 500 bar. The first injection start of command was at -324° ATDC and the second injection start of command was at -47° ATDC. The first injection timing is early in the intake stroke and it creates a homogenous, premixed charge of fuel and air. This was clearly demonstrated

with previous work by the authors [7]. The intake pressure and temperature were 1.16 bar and 26°C, respectively, with a cooled external EGR rate of 37%.

Figure 6 illustrates the combustion timing controllability results for this PFS strategy by varying the premixed fuel percentage from 100% (fully premixed with only the first injection) to 50%. Over this sweep the combustion efficiency remains essentially constant at 94% and the BSNOx emissions remain below 0.2 g/kW-hr for the premixed percentages of 60% and greater, but as the mixture becomes more stratified and combustion advances, the NOx emissions increase. The 50% premixed case has a BSNOx level of 0.45 g/kW-hr.

As illustrated, there is very little authority to control the timing of combustion via the fuel injection strategy, despite the fact that the fuel has a relatively low octane number and does display a two-stage ignition processes and low temperature heat release. The CA50 advances only ~3 crank angle degrees as the premixed ratio is reduced from 100% to 50%. The combustion phasing advances slightly because as the amount of DI fuel injected increases, the peak local equivalence ratio increases, and richer mixtures have shorter ignition delays. This is a large increase in fuel stratification, as indicated by the NOx emissions increase. However, despite the change in fuel stratification, the timing of combustion remains relatively unaffected. This is due to the competition between localized cooling due to the latent of vaporization of the DI fuel and the increase in reactivity due to the richer mixture.

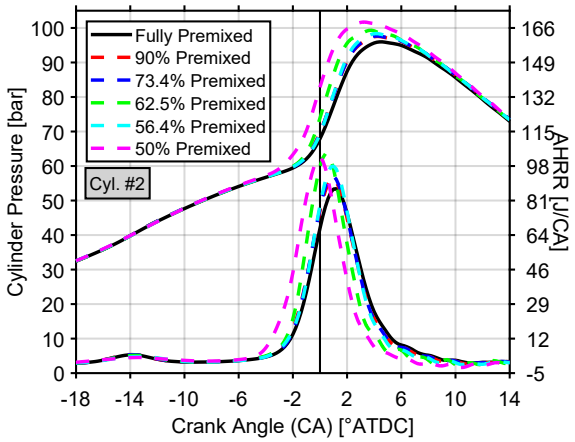

Figure 6: Combustion timing controllability results for PFS operation with the 68 RON gasoline at 2000 rpm, 4 bar BMEP.

These findings regarding PFS controllability are consistent with Dec et al. [4] and Dempsey et al. [6]. Essentially, at relatively low engine loads with low intake pressures (<~ 2 bar-a), the fuel's autoignition chemistry is not sensitive enough to partial equivalence stratification, which results in very little authority to control the ignition delay. Dec has shown that by using high intake pressures of 2 bar-a or greater, gasoline's autoignition chemistry can become quite sensitive to the equivalence ratio, thus providing a control mechanism via stratification. However, for light-duty engines and drive cycles, this level of intake pressure boosting is extremely taxing for the engine's air system and results in large parasitic losses, as shown in Dempsey et al. [7].

HFS operation uses no premixed fuel and direct injects the fuel near top dead center, much like a conventional diesel engine. Use of a single or multiple fuel injection strategy for HFS operation was investigated using the 68 RON gasoline at the same 2000 rpm, 4 bar BMEP operating condition studied with PFS, but with a slightly higher rail pressure of 640 bar, an intake pressure of 1.22 bar-a, an intake temperature of 65°C, and varying EGR levels. For the double injection strategy, ~10% of the total fuel mass is injected in the first injection. This was determined based on rate of injection measurements made the same model injector as used in this study [23]. As the EGR level was increased, the injection timing was advanced to maintain combustion phasing (CA50) at 8° ATDC. Figure 7 shows the two injection strategies and how they varied as the EGR level was varied.

Using the 68 RON gasoline, the single injection timing varied between -9° ATDC and -17° ATDC as the EGR level was increased from 5% to 40%. The double injection strategy features a pilot and a main with a fixed dwell of 0.82 ms. Over the same EGR sweep, the double injection strategy requires a main injection that is a few crank angle degrees retarded from the single injection strategy to maintain a CA50 of 8° ATDC. This suggests that the pilot injection reduces the ignition delay of the main injection, which is expected.

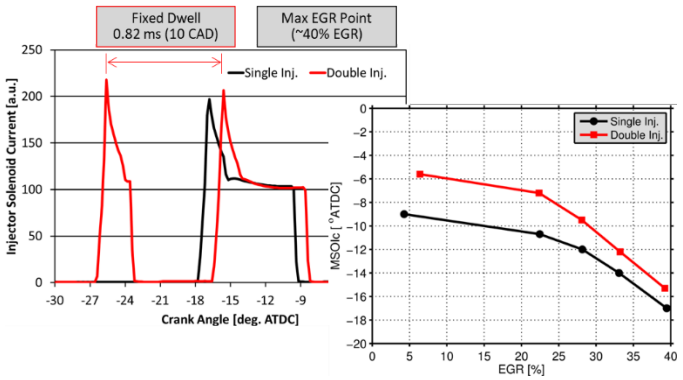

Figure 7: Single and double injection HFS operating strategies using the 68 RON gasoline at 2000 rpm, 4 bar BMEP. (Left) Injector solenoid current for the single and double injection strategy at the 40% EGR condition and (right) main injection start of current as the EGR level is varied. Double injection has a pilot with a constant advance of 0.82 ms.

Figure 8 shows a comparison of the combustion processes for the single and double injection HFS strategies at the lowest and highest EGR rate. At low EGR levels, the double injection strategy is useful for reducing the peak heat release rate, and thus the peak pressure rise rate and the combustion noise are reduced. At high EGR rates of 40%, the injections are sufficiently advanced that the effects of the pilot injection are "mixed-out" and diminished. The single and double injection combustion processes are almost identical at the higher EGR rates.

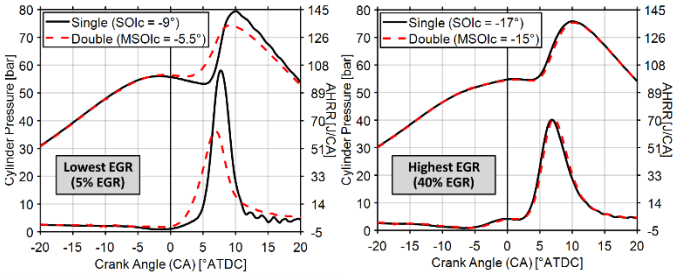

Figure 8: Comparison of the combustion process for single and double injection HFS operating strategies using the 68 RON gasoline at 2000 rpm, 4 bar BMEP at low EGR levels (left) and high EGR levels (right) with CA50 fixed at 8° ATDC.

Figure 9 shows the brake specific HC, CO, and NOx emissions for the single and double injection strategies over the EGR sweep. The unburned hydrocarbon emissions are relatively constant at ~2.5 g/kW-hr for both injection strategies and only increasing slightly at the highest EGR levels. At low EGR levels, the single injection strategy produces ~3x more CO emissions than the double injection strategy, which is likely due to over-mixing creating overly lean regions that do not burn to completion. This was conclusively shown for diesel LTC operation in an optical engine by Sahoo et al. [33] and Dempsey et al. [28]. As the EGR rate is increased, the CO emission increase dramatically, with the single and double injection strategies eventually converging.

As shown in Figure 9, the NOx emissions can be reduced dramatically by using large amounts of cooled EGR. At near zero EGR levels, the single injection strategy produces ~55% higher NOx emissions compared to the double injection. Again, at high EGR rates, the strategies converge and yield similar NOx emissions.

While not shown in the figure, soot emissions were measured over this EGR sweep. The single injection strategy had a peak soot level of 0.04 FSN at 40% EGR and the double injection strategy had a peak soot level of 0.14 FSN at 40% EGR. The only disadvantage of the double injection appears to be slightly elevated soot emissions, but, as will be shown in the next section, the double injection HFS-GCI soot levels are low relative to diesel fuel.

In summary, the double injection HFS strategy delivers excellent control authority with lower NOx, CO, and combustion noise compared to a single injection, with a minimal soot emissions penalty. Based on this, the double injection strategy for HFS-GCI operation will be used throughout the remainder of the study.

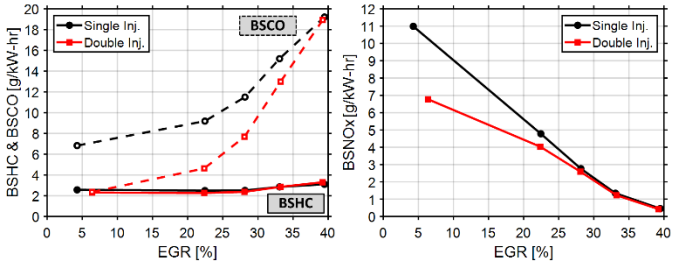

Figure 9: Comparison of the emissions for single and double injection HFS operating strategies using the 68 RON gasoline at 2000 rpm, 4 bar BMEP. (Left) Brake specific HC & CO and (right) brake specific NOx emissions as the EGR level is varied.

Using the same double injection strategy (Figure 7) with 27% EGR, a start of injection sweep was conducted to investigate the combustion timing controllability of HFS-GCI operation with the 68 RON gasoline. Figure 10 shows the results from three different main start of injection commands (MSOIc). Recall, the pilot injection moves with the main injection, holding a constant 0.82 ms dwell. As shown in the figure, the timing of combustion can readily be controlled by varying the injection timing, with earlier injections advancing combustion and vice versa, like conventional diesel combustion (CDC).

Figure 11 compares the results of the HFS-GCI timing sweep with the 68 RON gasoline to CDC at the same operating condition, using the same double injection strategy. The combustion timing control authority is very similar between the two fuels in this injection timing range. For the HFS-GCI operation, as the injection timing is retarded, the rate of CA50 retard increases compared to CDC. This is because the ignition delay is elongated due to the lower reactivity of the gasoline at the retarded injection timings and, because the piston is moving away at a faster rate, is more sensitive to changes in the MSOIc.

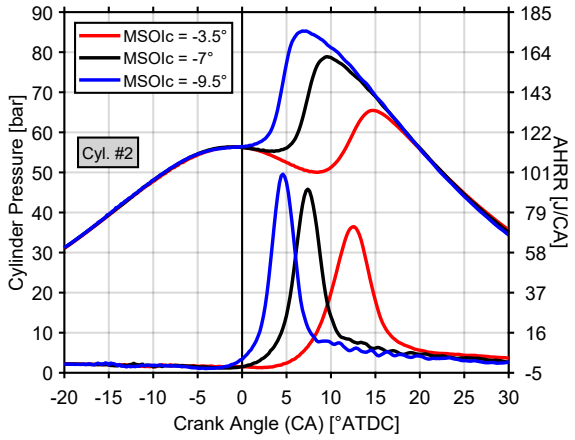

Figure 10: Combustion process for double injection HFS using the 68 RON gasoline with 27% EGR at 2000 rpm, 4 bar BMEP and varying the injection timing.

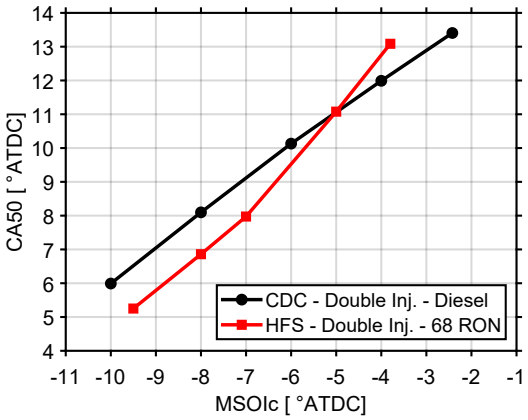

Figure 11: Combustion control authority of CDC vs. HFS-GCI with 68 RON gasoline using a double injection strategy with 27% EGR at 2000 rpm, 4 bar BMEP.

These experiments have clearly shown that HFS-GCI operation has a much higher level of combustion timing control authority compared to PFS-GCI operation. HFS-GCI operation has comparable control authority as conventional diesel using injection timing, which is a desirable trait. PFS-GCI operation typically uses a varying premixed fraction rather than injection timing to control combustion. As demonstrated previously, a 50% change in premix fraction only shifted combustion phasing by ~3 crank angle degrees.

Considering the controllability advantage of HFS-GCI operation compared to the more premixed strategies, the remainder of this study focuses on fuel reactivity effects of HFS-GCI operation with a double injection strategy on a production multi-cylinder light-duty compression ignition engine. The focus is on understanding if the production air handling system can achieve LTC operation by using moderate to large amounts of cooled EGR for a wide range of gasoline reactivities.

EXPERIMENTAL OPERATING CONDITIONS

HEAVY FUEL STRATIFICATION (HFS) OPERATION

The remainder of this study will focus on the engine performance and emissions implications of HFS-GCI operation with a wide range of gasoline reactivities, with comparisons made to conventional diesel fuel. The engine will be operated at two unique conditions: a 4 bar BMEP point and a 10 bar BMEP point. The conditions for each of these operating points is outlined in Table 3. For HFS-GCI operation and CDC operation, the exact same double injection strategy is used as outlined in Table 3, but with the injection timings adjusted to achieve the targeted CA50. The injection timings listed in Table 3 are start of injection command (SOIc). As mentioned previously in the experimental setup, the injection timing is trimmed slightly from cylinder-to-cylinder to achieve the desired CA50 target.

Table 3: Operating conditions for HFS-GCI operation with various gasoline fuels compared to diesel fuel.

Conditions	***4 bar BMEP***	***10 bar BMEP***
Speed [rpm]	2000	2000
Load (BMEP) [bar]	4.0 ± 0.1	10.0 ± 0.1
Int. Man. P [bar-a]	1.22 (Target)	1.75
Int. Man. T [°C]	32° (Target)	40°
External EGR [%]	0% to 55%	0%
Swirl ratio [-]	2.5 (60% Open VSA)	2.0 (100% Open VSA)
Pilot SOIc [°ATDC]	~ -40° to -13° (10° from Main)	~ -16° to -14° (10° from Main)
Pilot Fuel* [mass%]	~10%	~10%
Main SOIc [°ATDC]	~ -30° to -3° (Fixed CA50)	~ -6° to -4° (Fixed CA50)
Combustion Phasing (CA50) [°ATDC]	8°	10°
Rail Pressure [bar]	500 & 1000	1080

*Based on fuel injector characterization [23]

RESULTS

HFS FUEL EFFECTS – 4 BAR BMEP

At the mid-load 4 bar BMEP operating condition, a parametric variation in the EGR level was conducted while adjusting the injection timing to maintain CA50 at 8° ATDC. The total fueling rate is varied to maintain the engine output at 4 bar BMEP. Figure 12 shows the air handling system response and boundary pressure and temperatures on the engine as a result of the EGR sweep. For EGR levels of 30% and lower, the VGT can maintain the target intake manifold pressure of 1.22 bar-a. It does this by generating a restriction and increasing the velocity across the turbine. However, this tends to increase the exhaust manifold pressure, which in turn increases the pumping losses, as illustrated by Kodebyle Raju et al. [34]. As the EGR level is increased beyond 30%, the VGT is at its maximum restriction and is unable to maintain the target intake pressure, which begins to drop as EGR increases further. At the maximum EGR rate of 55%, the intake pressure has dropped to ~1.07 bar-a. Once the VGT has reached its maximum restriction at 30% EGR, the exhaust manifold pressure decreases as well with increasing EGR rate.

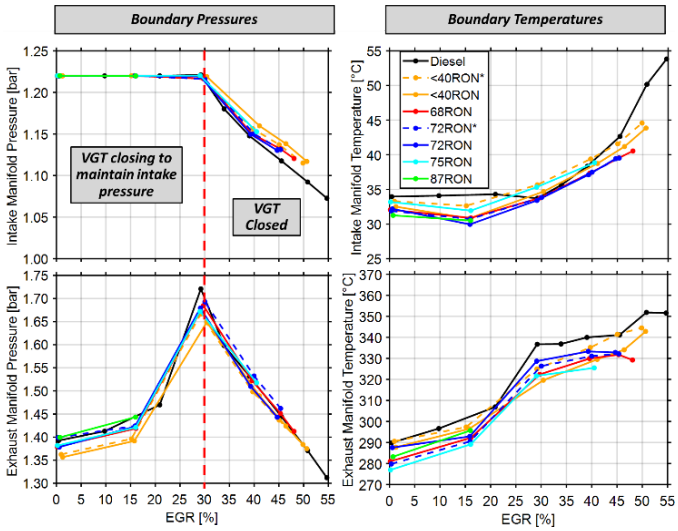

Figure 12: Air handling response over the parametric variation of the EGR rate at the 4 bar BMEP condition.

Figure 12 also shows the manifold temperatures response to the EGR variation. The CAC and EGR cooler had 30°C water flowing through them throughout the sweep, to maintain low and steady intake temperatures near 32°C. The authors realize that the intake temperatures used here are likely unrealistically low for a production engine, particularly with large amounts of EGR. However, the goal was to demonstrate ultra-low NOx and soot emissions with HFS-GCI operation, and thus the intake temperature was reduced as much as possible in the laboratory. As shown in the figure, there is day-to-day variation in the intake temperature amongst the fuels and as the EGR rate is increased, an intake temperature of 32°C was not maintained. However, the increase in intake temperature with EGR rate is consistent amongst all the fuels. The exhaust manifold temperature monotonically increases with EGR rate, but from an exhaust thermal management perspective, it is important to realize that the exhaust mass flowrate reduces with increasing EGR rate.

Figure 13 shows the how the molar intake oxygen concentration and global equivalence ratio vary over the EGR sweep. At the highest EGR level of 55%, the intake oxygen concentration has reduced to ~10% and the global equivalence ratio has increased to ~0.8, from its baseline of ~0.3 at 0% EGR. This is one of the defining aspects of this work. In many engine combustion research studies using single-cylinder engines, large amounts of EGR are used, but while maintaining a very lean overall equivalence ratio, by adding air and EGR simultaneously. However, in a production multi-cylinder engine, with specific turbomachinery, this is very difficult to achieve, as illustrated here.

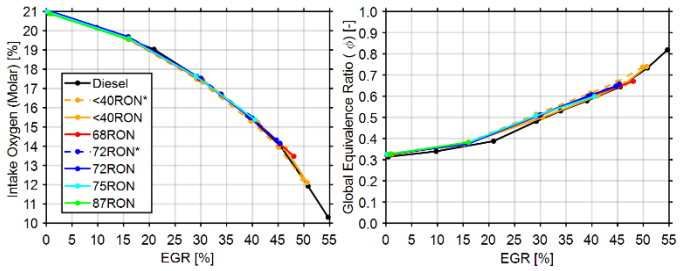

Figure 13: Intake oxygen and global equivalence ratio over the parametric variation of EGR rate at the 4 bar BMEP condition.

Figure 14 shows how the injection timing varies to maintain fixed combustion phasing as the EGR rate is increased using the various fuels with 500 bar and 1000 bar rail pressure. Diesel fuel was only operated at the 1000 bar rail pressure due to excessively high soot emissions with the lower rail pressure of 500 bar. As shown in the figure, as the EGR rate is increased, the injection timing was advanced considerably to maintain CA50 at 8° ATDC. It is tempting to state that the ignition delay is longer for the lower rail pressure, because an earlier MSOIc was required to maintain combustion phasing. However, it is important to keep in mind that these are start of injection commands and unfortunately, a full hydraulic characterization of these injectors with these fuels has not been conducted. Therefore, it is not advisable to compare ignition delays in detail currently.

Figure 14 does clearly show that the lower injection pressure increases the EGR tolerance for the lower reactivity (higher octane number of 72 RON and higher) gasoline fuels. This is thought to be due to locally richer conditions that serve as a stronger and more stable ignition source for early injection timings. However, as will be shown in a subsequent section, there is a detrimental effect on soot emissions with the lower injection pressure.

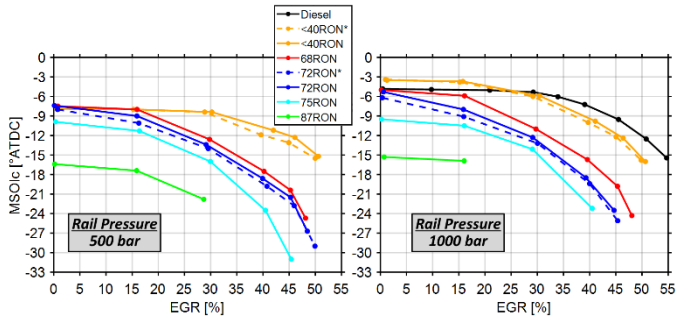

Figure 14: Main start of injection command (MSOIc) variations using the double injection strategy at (left) 500 bar and (right) 1000 bar rail pressure over the parametric variation of the EGR rate at the 4 bar BMEP condition.

The higher octane gasolines, particularly the 75 and 87 RON fuels, were unable to operate at the highest EGR levels of greater than 40%. The lower rail pressure helped with this, but not completely. The limiting factor that determined the max allowable EGR level was not cyclic variability, as might be expected, but rather due to a cylinder-to-cylinder imbalance in the combustion phasing. The engine's high pressure loop EGR

system, illustrated in Figure 2, has cylinder #4 closest to the EGR valve and it is theorized that cylinder #4 receives more EGR than the other 3 cylinders. This maldistribution of EGR is likely occurring at all EGR levels, but with independent control over each cylinders SOI timing and fueling, it is easily corrected by adjusting the injection timing (± ~1 to 3 CAD). However, when the EGR rate exceeds ~40%, no amount of variation in the injection timing could correct for the EGR maldistribution with the higher octane gasolines fuels.

To understand why this was occurring, CFD modeling was used. In the CFD model, the 4 bar BMEP condition was simulated with the same double injection strategy outlined in Table 3, using a rail pressure of 1000 bar. In the simulations, main injection timing sweeps were conducted at three different EGR levels: 30%, 48%, and 51%. This was done for CDC operation with diesel fuel, which was simulated as tetradecane physically and n-heptane chemically, and for HFS-GCI operation with the 68 RON gasoline, which was simulated as iso-octane physically and PRF68 chemically. PRF68 is 68% iso-octane and 32% n-heptane by volume. The physical fuel surrogate is chosen based on properties of the liquid fuel such as density, viscosity, volatility, and heat of vaporization. The chemical fuel surrogate is chosen based on chemical reactivity in the gas phase. For more details on the CFD modeling setup, please refer to Dempsey et al. [1]. The results from the CFD study are illustrated in Figure 15.

Just as in the experiments, diesel fuel is very tolerant of EGR from a standpoint of combustion timing controllability and requires only minor changes to the injection timing to maintain a given CA50 if the EGR level is perturbed. Thus, it is easy to correct for the cylinder #4 EGR maldistribution by simply advancing the injection timing slightly when operating with diesel fuel at high EGR levels.

However, with PRF68 fuel (simulating the base 68 RON gasoline fuel), the results are quite different. When the EGR rate is 30% or lower, the HFS-GCI combustion timing controllability is pronounced and monotonic. However, as the EGR level increases to 48%, the authority over combustion timing via the injection timing has diminished. At 51% EGR, the combustion phasing begins to retard, and it is not possible, with any injection timing to achieve a CA50 earlier than 8° ATDC. An injection timing of ~-27° ATDC yields the most advanced combustion but advancing or retarding the injection timing from here results in delayed combustion.

In the experiments, when the engine is at a nominal EGR level, it is likely that cylinder #4 is receiving a higher EGR level. Thus, when the nominal EGR level approaches 40%, even though the combustion phasing in the front three cylinders can be controlled via the injection timing, the combustion phasing of cylinder #4 is delayed later than 8° ATDC and unrecoverable. This is the limiting factor that determined the max EGR level for the higher octane number gasolines in this study. Thus, if HFS-GCI is to be implemented in a production engine with high pressure loop EGR, it is important that the EGR distribution in the intake be uniform. This is especially true if the goal is to achieve LTC operation, which will require large amounts of EGR.

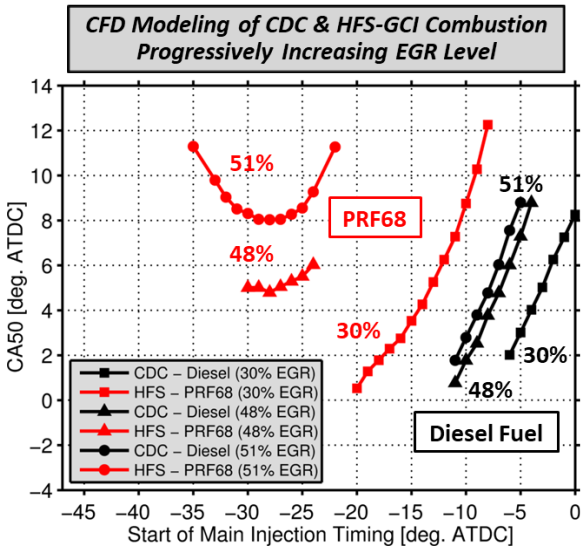

Figure 15: CFD modeling results at the 4 bar BMEP operating condition for CDC (diesel fuel) and HFS-GCI (PRF68) with a rail pressure of 1000 bar, both using a double injection strategy.

Taking a closer look at the experimental results, Figure 16 shows the ensemble averaged cylinder pressure and AHRR from cylinder #2 for CDC operation with diesel fuel and HFS-GCI with the 68 RON gasoline, both using a rail pressure of 1000 bar. At low EGR levels, the HFS-GCI strategy has higher peak heat release rates, but at the high EGR levels, the combustion processes are similar, in terms of peak heat release rate and combustion duration. This is very interesting, because at low EGR levels, the injection timings are similar for these two fuels, but at high EGR levels, the injection timings are significantly different.

These results suggest that fuel volatility is playing a significant role, particularly at the low EGR levels. The 68 RON gasoline evaporates more readily than the diesel fuel, thus, when the ignition delays are similar, it is expected that the gasoline fuel will have more charge prepared to ignite and participate in the initial heat release, leading to a higher peak heat release rate compared to the less volatile diesel fuel. At the higher EGR levels, it is suspected that the injection timings are so advanced, that these differences mix out, leading to very similar heat release rates between the 68 RON fuel and the diesel fuel.

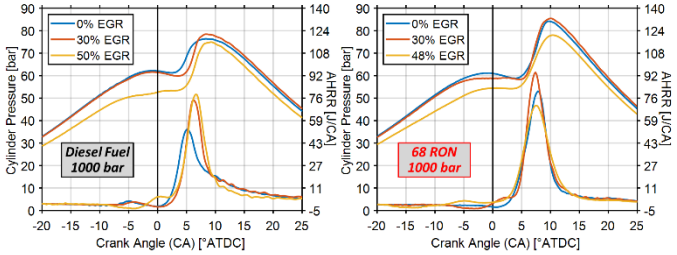

Figure 16: Ensemble averaged cylinder pressure and AHRR from cylinder #2 for CDC and HFS-GCI operation with the 68 RON gasoline at the 4 bar BMEP operating condition.

Figure 17 shows the gross cycle indicated efficiency (GIE), the net cycle indicated efficiency (NIE), and the brake thermal efficiency (BTE) over the parametric variation of EGR rate at the 2000 rpm, 4 bar BMEP condition, using a rail pressure of 1000 bar. Note, all fuels shown here are using the double injection strategy outlined in Table 3 and the injection timing is being adjusted to maintain CA50 at 8° ATDC.

The GIE is relatively constant, but increasing slightly as the EGR rate increases. This is likely due to reductions in the in-cylinder heat transfer losses stemming from lower combustion temperatures as the EGR rate is increased. Across the entire EGR sweep, all the gasoline fuels have lower GIE than diesel fuel. This is due to lower combustion efficiency (i.e., higher CO and UHC emissions) with the gasoline fuels and potentially higher in-cylinder heat transfer losses. This is thought to be a potential factor because the NOx emissions are higher for the gasoline fuels, which means that there is more cylinder mass at high temperature, which could increase heat transfer losses. Both the combustion efficiency and the NOx emissions will be shown in subsequent figures. These trends in GIE between gasoline fuels and diesel fuel using HFS operation with large amounts of EGR on a light-duty engine have been shown by previously by Solaka et al. [35]. They also attributed the lower GIE to combustion inefficiencies and heat transfer losses.

Adding the exhaust and intake strokes, takes the data from the gross cycle to the net cycle. Due to elevated exhaust manifold pressures created by the VGT, the pumping losses are increased and the NIE is reduced considerably going from 0% to 30% EGR. Beyond 30% EGR, the VGT is at maximum restriction and the NIE increases again, due to the GIE increasing and the exhaust manifold pressure decreasing (as shown in Figure 12).

The difference between the NIE and the BTE is essentially constant for a given fuel over the EGR sweep. This is expected considering the friction and parasitic losses of the engine are mainly a function of engine speed, which is constant at 2000 rpm. However, it is worth noting that the difference between NIE and BTE for the gasoline fuels is slightly greater than with diesel fuel. This suggests that there are high parasitic losses when the engine is fueled with gasoline. The authors speculate that it is due to high losses in the high pressure common rail pump, which is driven off the engine's crankshaft. The viscosity of the gasoline fuels is significantly lower than diesel fuel, thus there could be high leakage in the compression chambers of the high pressure pump. Additionally, the bulk modulus of gasoline is lower than that of diesel fuel. These two properties, lower viscosity and lower bulk modulus, suggest that more work would need to be supplied to the high pressure pump to achieve a given rail pressure for a gasoline fuel, increasing the parasitic losses and decreasing the BTE relative to diesel fuel, for a given NIE.

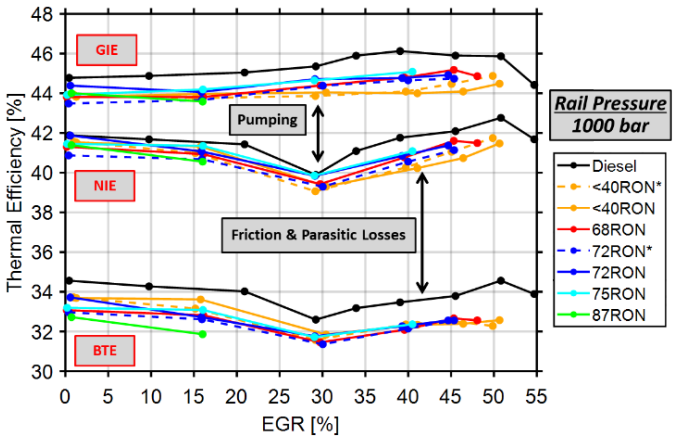

Figure 17: Thermodynamic engine efficiencies at the 4 bar BMEP operating condition over the parametric variation of EGR using a fuel rail pressure of 1000 bar.

Figure 18 shows the thermodynamic engine efficiencies using a common rail fuel pressure of 500 bar for the gasoline fuels. The diesel fuel was not run at this low rail pressure due to excessively high soot, but the 1000 bar operation with diesel fuel is shown for reference. The results at the lower fuel rail pressure are quite similar, with two important differences.

First, the difference between the NIE and BTE of the gasoline fuels is very similar to diesel fuel at the 1000 bar condition. This is particularly evident and easy to visualize at the low EGR levels when all the fuels have high combustion efficiency. This suggests that there are less parasitic losses for the gasoline fuels at 500 bar than at 1000 bar, lending credence to the speculation that the additional parasitic for gasoline fuels at high injection pressures stems from the high pressure common rail pump.

Second, the higher octane gasoline fuels (68 RON and higher) yield low GIE with high EGR levels, beyond 30% EGR. This is clearly due to poor combustion efficiency, which will be shown in subsequent figure. The very low octane gasolines (<40 RON) yield near diesel GIE, NIE, and BTE across the EGR sweep with the lower injection pressure of 500 bar.

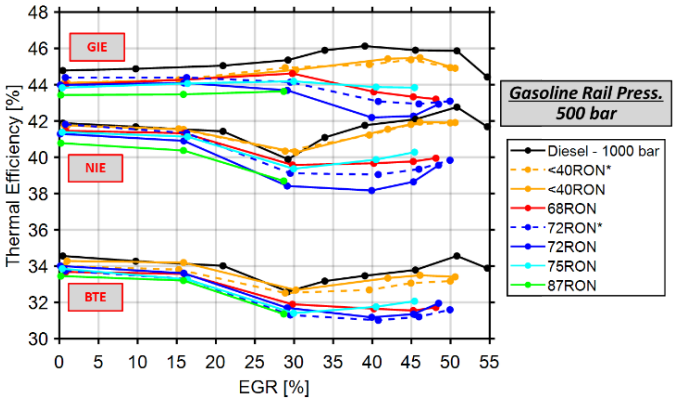

Figure 18: Thermodynamic engine efficiencies at the 4 bar BMEP operating condition over the parametric variation of EGR using a fuel rail pressure of 500 bar for the gasoline fuels and 1000 bar for diesel fuel.

Figure 19 shows the combustion efficiency for the 500 bar and 1000 bar rail pressure conditions. Diesel fuel yields the highest combustion efficiency, which results in the highest GIE, as shown previously. For the gasoline fuels, the combustion efficiency is reasonably good at the higher injection pressure, staying at 97% and above, except for the 87 RON fuel, which suffers from early injections and significant over-leaning in-cylinder. However, when the injection pressure is reduced to 500 bar, the combustion efficiency of the gasoline fuels reduces considerably, particularly at high EGR levels. Essentially, the higher injection pressure is required to improve mixing in the low oxygen environment of highest EGR levels. Recall, that at the highest EGR levels the global equivalence ratio is approaching ~0.8, and thus in-cylinder oxygen is limited.

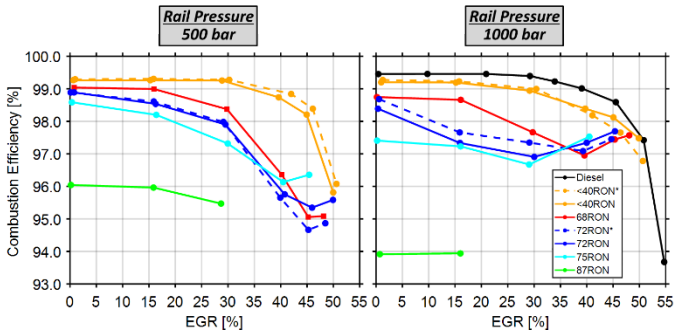

Figure 19: Combustion efficiencies at the 4 bar BMEP operating condition over the parametric variation of EGR using a fuel rail pressures of 500 and 1000 bar.

Figure 20 shows the BSNOx emissions with the rail pressure set at 1000 bar. At the low EGR levels, the NOx emissions increase as the octane number increases. This is due to the more advanced injection timings, which results in a high peak heat release rate and likely more cylinder mass at a near stoichiometric equivalence ratio, producing high local temperatures. This trend does break down for the highest octane, 87 RON fuel, suggesting that the injection timing was advanced enough for this fuel, such that the near stoichiometric regions had enough time to mix out to leaner conditions. As the EGR level is increased, the NOx emissions decrease, as expected. The fuels with the EHN additive (indicated by an asterisk) have higher NOx emissions than their counterpart fuel with the same RON, which had the DTBP additive. This has been shown in several studies and stems from the fuel bound nitrate group in the EHN molecule [30], [31], [36]. The NOx emissions can only be reduced to below ~0.2 g/kW-hr for EGR rates above ~50% for the non-EHN containing fuels.

This suggests that HFS-GCI strategies will likely require lean NOx aftertreatment, regardless of the gasoline reactivity. Figure 21 shows the NOx emissions for the gasoline fuels at 500 bar injection pressure and the results are very similar, but with slightly reduced NOx levels at a given EGR level. However, it is clear, that using lower injection pressure will not be the key to achieving ultra-low NOx levels and removing the need for NOx aftertreatment, at least with an air handling arrangement consistent with the one used on this test engine.

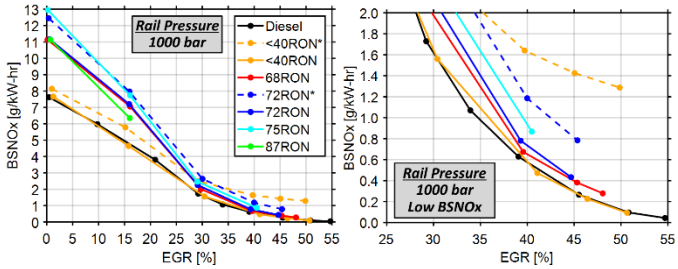

Figure 20: Brake specific NOx (BSNOx) emissions at the 4 bar BMEP operating condition over the parametric variation of EGR using a fuel rail pressure of 1000 bar.

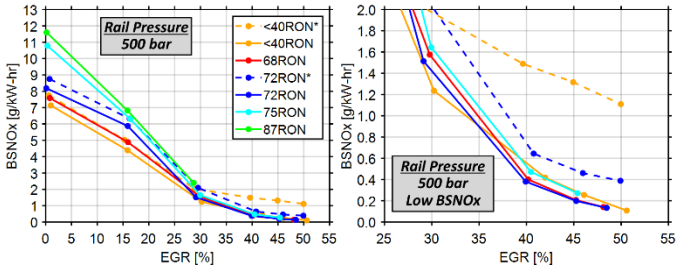

Figure 21: Brake specific NOx (BSNOx) emissions at the 4 bar BMEP operating condition over the parametric variation of EGR using a fuel rail pressure of 500 bar.

Figure 22 shows the soot (black carbon) emissions as measured by an AVL 415S smokemeter using a rail pressure of 1000 bar. Using diesel fuel, the soot emissions are lowest at 0% EGR, with an FSN of ~0.2, and continually increase to an FSN over 2.0 at ~55% EGR. The gasoline fuels at the higher injection pressure all produce very low soot emissions, with FSN levels of essentially zero, except for the <40 RON fuels, which have a peak FSN of ~0.05. It is interesting to note that the <40 RON fuel with DTBP (non-asterisk) had very similar injection timings compared to diesel fuel (Figure 14) and very similar NOx emissions (Figure 20), but has significantly lower soot emissions. The authors suspect that the higher volatility of the

gasoline fuel is the dominant factor, but this will require further investigation to be proven conclusively. Another potential factor is the chemical makeup of the fuel (e.g., lower aromatic content, lower polycyclic aromatic content, and higher hydrogen-to-carbon ratio). The authors feel that this could play a role and further investigation is needed to understand primary factor.

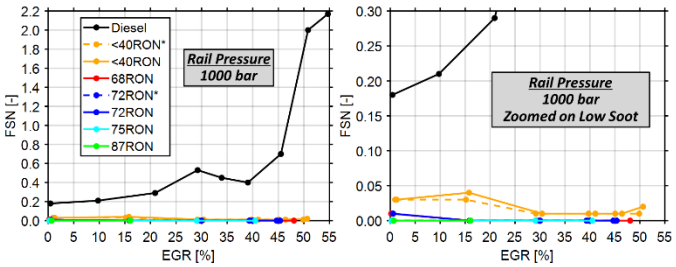

Figure 22: Filter Smoke Number (FSN) at the 4 bar BMEP operating condition over the parametric variation of EGR using a fuel rail pressure of 1000 bar.

Figure 23 shows the soot emissions for the gasoline fuels at the lower rail pressure of 500 bar. For the lowest octane fuels, the soot emissions are significantly higher, but for the 75 and 87 RON fuels, the soot emissions remain near zero FSN. For the intermediate octane fuels (68 and 72 RON), the soot emissions trend is very characteristic of what has been observed with heavy EGR diesel engines (i.e., diesel PCCI). As the EGR rate is progressively increased and the injection timing advanced to maintain combustion phasing, the soot emissions increase to a point and then decrease dramatically. This occurs when the fuel injection event ends prior to the start of combustion and the peak flame temperatures are low enough to suppress soot formation. With diesel fuel, this has been shown to occur at EGR rates of 60% to 75%, depending on engine load [37], [38]. In this study, this did not occur with diesel fuel because we were unable to use high enough EGR rates (greater than 55%), before the overall air/fuel ratio approached stoichiometric. However, as shown in Figure 23, this was achieved with the 68 and 72 RON gasoline fuels at ~45% EGR. This highlights one of the primary advantages of using a lower reactivity fuel, such as gasoline, rather than diesel fuel for LTC operation.

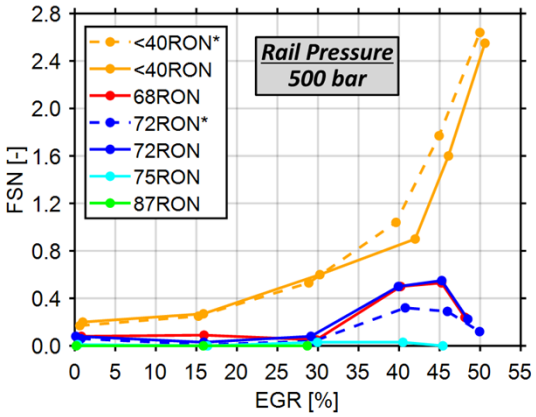

Figure 23: Filter Smoke Number (FSN) at the 4 bar BMEP operating condition over the parametric variation of EGR using a fuel rail pressure of 500 bar.

RESULTS

HFS FUEL EFFECTS – 10 BAR BMEP

In addition to the 4 bar BMEP condition, a second operating condition was investigated to demonstrate the fuel effects of HFS-GCI operation at higher loads. The study was not exhaustive, and only a single operating point was studied with each fuel. This was done to demonstrate that high load, mixing controlled combustion with gasoline fuels in a modern compression ignition engine is easily achieved. The focus was not on achieving LTC operation.

The fixed operating conditions of this 10 bar BMEP point are shown in Table 3. Table 4 shows the results of the single 10 bar BMEP operating point for each fuel. The main start of injection command (MSOIc) was adjusted to maintain CA50 at 10° ATDC. All the fuels required a similar MSOIc to achieve the desired CA50. At higher engine loads, the in-cylinder pressure and temperatures are sufficiently high that fuel reactivity differences tend to be diminished, as shown by Paz et al. [39].

Table 4: Experimental results at the 10 bar BMEP condition.

		Gasoline Fuels						
Results	**Diesel**	**<40RON***	**<40RON**	**68RON**	**72RON***	**72RON**	**75RON**	**87RON**
MSOIc [°ATDC]	-5.4	-4.8	-4.7	-4.7	-4.7	-4.7	-4.7	-4.5
GIE [%]	46.1%	45.2%	45.3%	45.1%	44.7%	44.5%	44.9%	44.9%
NIE [%]	43.8%	43.0%	43.1%	42.8%	42.3%	42.2%	42.8%	42.8%
BTE [%]	40.2%	39.2%	39.4%	39.1%	38.9%	38.6%	38.9%	39.1%
BSNOx [g/kW-hr]	8.2	8.4	8.6	8.2	9.2	8.7	8.0	8.3
FSN [-]	0.1	0.03	0.03	0.02	0.02	0.02	0.02	0.02
Comb. Eff. [%]	99.7%	99.7%	99.7%	99.7%	99.7%	99.7%	99.7%	99.7%

The ensemble averaged cylinder pressure and AHRR are shown in Figure 24. As shown in the figure, the initial combustion process is very different amongst all the fuels. This is known as the premixed portion of the mixing controlled combustion event, and, due to the varying fuel reactivities, it is

logical that this stage of the combustion process would be different amongst these fuels. The diesel fuel ignites almost instantaneously under these conditions and has no evidence of premixed combustion event and quickly transitions into a mixing controlled combustion process. Because of this behavior, it required a slightly earlier MSOIc compared to the gasoline fuels to achieve a CA50 of 10° ATDC, due to its combustion process starting earlier.

The gasoline fuels all have essentially the same MSOIc and exhibit a premixed combustion event, sometimes referred to a "premixed spike". The amount of energy released during this phase is proportional to the ignition delay, which is approximately proportional to the octane number of the fuel. The <40 RON gasoline fuels tend to have a small premixed combustion event and the 87 RON fuel has the largest premixed event, with the energy release exceeding the peak mixing controlled heat release rate of the other fuels (which occurs ~9 to 11° ATDC).

It is interesting to note that the two fuels with 72 RON have significantly different ignition delays and premixed heat release rates. This suggests that the conventional RON test might not adequately predict the performance of a gasoline fuel for HFS-GCI operation. This is a potentially important research topic for the fuels and combustion community to investigate in the future if HFS-GCI engines are of interest.

After the premixed portion of the heat release is complete, all the fuels transition to a mixing controlled combustion process, which is governed by fuel/air mixing. The mixing rate, and thus the heat release rate, is controlled by the fuel injection rate, the bowl shape, bulk gas motion, and the local turbulence level. It is not expected that these factors would be fuel specific and thus it is not surprising to see the mixing controlled portion of the heat release (from ~10° to 35° ATDC) be identical for all the fuels.

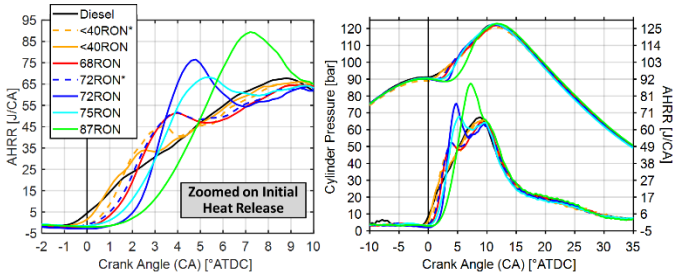

Figure 24: Ensemble averaged cylinder pressure and AHRR from cylinder #2 for 10 bar BMEP operation. (Right) AHRR plots focused on the initial heat release and (left) cylinder pressure & AHRR for the entire combustion event.

As shown in Table 4, the gasoline fuels yield similar NOx emissions compared to diesel fuel, but with a reduction in soot emissions. All fuels have equal combustion efficiency at 99.7%, but operation with diesel fuel yields higher GIE, NIE, and BTE by ~1% absolute, compared to the gasoline fuels. This is thought to be due to high heat transfer losses in-cylinder when using the gasoline fuels. The higher premixed heat release rate could tend to increase local gas temperatures and induce pressure oscillations in-cylinder. These pressure oscillations have been shown to increase heat transfer losses [40].

CONCLUSION & SUMMARY

In this work, a light-duty multi-cylinder engine was used to investigate the potential of GCI as an advanced combustion mode to achieve high efficiency and low emissions relative to diesel fuel. A wide variety of gasoline boiling range fuels was investigated, which had fuel reactivities that ranged from diesel -like, with RON less than 40, up to near market gasoline with a RON of 87. Thus, these fuels would be classified as low octane gasolines.

First it was highlighted that PFS operation, while it yields high efficiency and near zero NOx and soot emissions, has little authority over the timing of combustion at conditions relevant to light-duty drive cycles. On the contrary, it was shown that HFS operation has pronounced, diesel-like authority over the combustion timing via the fuel injection timing. This is a mandatory characteristic of any production viable advanced combustion strategy. Thus, the focus of this work was to study the impact of gasoline reactivity on HFS-GCI operation. The findings can be summarized as follows:

Mid-Load: 4 bar BMEP

1. HFS-GCI operation has diesel-like controllability over the combustion timing with significant reductions in soot emissions compared to diesel fuel.
2. Depending on the gasoline's reactivity and injection pressure, simultaneous ultra-low NOx and soot emissions (i.e., LTC) can be achieved, but only at high EGR rates of ~45% to 50%. This was achieved for low to moderate RON gasolines (<70 RON) with high injection pressure (1000 bar).
3. The higher octane fuels were unable to achieve LTC due to the EGR maldistribution with the high pressure loop EGR configuration of this particular test engine. The injections become so far advanced at high EGR rates that cylinder #4 was too delayed and unrecoverable. A more uniform EGR distribution would likely alleviate this issue and allow the higher octane fuels to use higher EGR levels and achieve LTC operation.
4. CFD modeling showed that diesel fuel is tolerant to the EGR maldistribution and slight adjustments can be made to the injection timing to achieve the desired CA50, even in the heavy EGR cylinder #4. However, the higher octane gasolines use much earlier injection timings and under heavy EGR conditions become overmixed and unable to correct for the EGR maldistribution via injection timing.
5. Lowering the injection pressure tended to improve the EGR tolerance of the gasoline fuels, however, the soot emissions increased dramatically, particularly for the lowest octane fuels (<40 RON).
6. At the mid-load operating condition, diesel fuel resulted in higher GIE, and thus higher NIE and BTE. The

higher GIE was due primarily to higher combustion efficiency with diesel fuel, but there was evidence that heat transfer losses could be higher with the gasoline fuels as well. Additionally, there were subtly higher parasitic losses with the gasoline fuels and it is suspected that these stem from higher leakage in the higher pressure fuel pump.

High-Load: 10 bar BMEP

1. At a higher engine load, the fuel reactivity differences are diminished, and all the fuels require very similar injection timings for mixing controlled combustion operation with a fixed CA50.
2. The magnitude of the premixed heat release rate is impacted significantly by the fuel reactivity, but the mixing controlled portion of the heat release rate is unaffected.
3. The gasoline fuels yield a soot emissions reduction at equal NOx levels at the high-load operating condition.
4. At the high-load condition, the GIE with diesel fuel was ~1% absolute higher than all the gasoline fuels, despite the combustion efficiencies being equal. This likely stems from higher heat transfer losses for the gasoline fuels during the premixed portion of the heat release, which tends to be higher for the gasoline fuels.

FUTURE WORK

Utilizing HFS-GCI combustion appears to be a promising and controllable advanced combustion strategy for future engines. At high-loads, conventional mixing controlled combustion can be used and there are significant soot benefits. At mid-load, LTC operation can be achieved, and this window of LTC operation could likely be expanded with an advanced air system and uniform EGR distribution. This engine would require modern SCR technology for lean NOx aftertreatment at high-load, but the drive cycle urea consumption could be reduced significantly. The soot emissions reduction shown here with HFS-GCI compared to diesel fuel could potentially result in an engine system that does not require active particulate filter regeneration, which will improve the overall system efficiency.

The biggest challenges for a GCI engine are startability and stable low-load operation. The engine research community and industry needs technologies and combustion strategies for stable and robust low-load operation (2 bar BMEP and below) for future GCI engines.

ACKNOWLEDGEMENTS

This research was supported by the DOE Office of Energy Efficiency and Renewable Energy (EERE), Vehicle Technologies Office and used resources at the National Transportation Research Center, a DOE-EERE User Facility at Oak Ridge National Laboratory. The authors would gratefully like to thank the U.S. DOE Vehicle Technologies Office Program Managers Kevin Stork and Gurpreet Singh for the support and guidance for this work.

REFERENCES

[1] A. B. Dempsey, S. J. Curran, and R. M. Wagner, "A perspective on the range of gasoline compression ignition combustion strategies for high engine efficiency and low NOx and soot emissions: Effects of in-cylinder fuel stratification," *Int. J. Engine Res.*, vol. 17, no. 8, 2016, doi: 10.1177/1468087415621805.

[2] M. Sjöberg, L. Edling, T. Eliassen, L. Magnusson, and H. Angström, "GDI HCCI : Effects of Injection Timing and Air Swirl on Fuel Stratification, Combustion and Emissions Formation," *SAE Technical Paper 2002-01-0106*. 2002, doi: 10.4271/2002-01-0418.

[3] J. E. Dec and M. Sjöberg, "Isolating the Effects of Fuel Chemistry on Combustion Phasing in an HCCI Engine and the Potential of Fuel Stratification for Ignition Control," *SAE Technical Paper 2004-01-0557*. 2004, doi: 10.4271/2004-01-0557.

[4] J. E. Dec, Y. Yang, and N. Dronniou, "Boosted HCCI - Controlling Pressure-Rise Rates for Performance Improvements using Partial Fuel Stratification with Conventional Gasoline," *SAE Int. J. Engines*, vol. 4, no. 1, pp. 1169–1189, 2011, doi: 10.4271/2011-01-0897.

[5] P. Loeper *et al.*, "Experimental Investigation of Light-Medium Load Operating Sensitivity in a Gasoline Compression Ignition (GCI) Light-Duty Diesel Engine," *SAE Technical Paper 2013-01-0896*. 2013, doi: 10.4271/2013-01-0896.

[6] A. B. Dempsey, N. R. Walker, E. Gingrich, and R. D. Reitz, "Comparison of low temperature combustion strategies for advanced compression ignition engines with a focus on controllability," *Combust. Sci. Technol.*, vol. 186, no. 2, 2014, doi: 10.1080/00102202.2013.858137.

[7] A. B. Dempsey, S. Curran, R. Wagner, and W. Cannella, "Effect of premixed fuel preparation for partially premixed combustion with a low octane gasoline on a light-duty multicylinder compression ignition engine," *J. Eng. Gas Turbines Power*, vol. 137, no. 11, 2015, doi: 10.1115/1.4030281.

[8] M. Sellnau, J. Sinnamon, K. Hoyer, and H. Husted, "Gasoline Direct Injection Compression Ignition (GDCI) - Diesel-like Efficiency with Low CO2 Emissions," *SAE Int. J. Engines*, vol. 4, no. 1, pp. 2010–2022, 2011, doi: 10.4271/2011-01-1386.

[9] M. C. Sellnau, J. Sinnamon, K. Hoyer, and H. Husted, "Full-Time Gasoline Direct-Injection Compression Ignition (GDCI) for High Efficiency and Low NOx and PM," *SAE Int. J. Engines*, vol. 5, no. 2, pp. 300–314, 2012, doi: 10.4271/2012-01-0384.

[10] Y. Ra *et al.*, "Gasoline DICI Engine Operation in the LTC Regime Using Triple-Pulse Injection," *SAE Int. J. Engines*, vol. 5, no. 3, pp. 1109–1132, Apr. 2012, doi: 10.4271/2012-01-1131.

[11] S. Tanov, R. Collin, B. Johansson, and M. Tuner,

"Combustion Stratification with Partially Premixed Combustion, PPC, using NVO and Split Injection in a LD - Diesel Engine," *SAE Int. J. Engines*, vol. 7, pp. 1911–1919, 2014, doi: 10.4271/2014-01-2677.

[12] A. B. Dempsey, B. Das Adhikary, S. Viswanathan, and R. D. Reitz, "Reactivity Controlled Compression Ignition (RCCI) using premixed hydrated ethanol and direct injection diesel," in *American Society of Mechanical Engineers, Internal Combustion Engine Division (Publication) ICE*, 2011, doi: 10.1115/ICEF2011-60235.

[13] G. T. Kalghatgi, P. Risberg, and H.-E. Angstrom, "Advantages of Fuels with High Resistance to Auto-ignition in Late-injection, Low-temperature, Compression Ignition Combustion," *SAE Technical Paper 2006-01-3385*. 2006, doi: 10.4271/2006-01-3385.

[14] V. Manente, B. Johansson, and P. Tunestal, "Partially Premixed Combustion at High Load using Gasoline and Ethanol, a Comparison with Diesel," *SAE Technical Paper 2009-01-0944*. 2009, doi: 10.4271/2009-01-0944.

[15] R. Hanson, D. Splitter, and R. D. Reitz, "Operating a Heavy-Duty Direct-Injection Compression-Ignition Engine with Gasoline for Low Emissions," *SAE Technical Paper 2009-01-1442*. 2009, doi: 10.4271/2009-01-1442.

[16] V. Manente, B. Johansson, P. Tunestal, and W. Cannella, "Effects of Ethanol and Different Type of Gasoline Fuels on Partially Premixed Combustion from Low to High Load," *SAE Technical Paper 2010-01-0871*. 2010, doi: 10.4271/2010-01-0871.

[17] H.-W. Won, N. Peters, N. Tait, and G. Kalghatgi, "Sufficiently premixed compression ignition of a gasoline-like fuel using three different nozzles in a diesel engine," *Proc. Inst. Mech. Eng. Part D J. Automob. Eng.*, vol. 226, no. 5, pp. 698–708, Oct. 2011, doi: 10.1177/0954407011423453.

[18] G. T. Kalghatgi, L. Hildingsson, A. J. Harrison, and B. Johansson, "Autoignition quality of gasoline fuels in partially premixed combustion in diesel engines," *Proc. Combust. Inst.*, vol. 33, no. 2, pp. 3015–3021, Jan. 2011, doi: 10.1016/j.proci.2010.07.007.

[19] J. J. López, J. M. García-Oliver, A. García, and V. Domenech, "Gasoline effects on spray characteristics, mixing and auto-ignition processes in a CI engine under Partially Premixed Combustion conditions," *Appl. Therm. Eng.*, vol. 70, no. 1, pp. 996–1006, Sep. 2014, doi: 10.1016/j.applthermaleng.2014.06.027.

[20] M. Wang, H. Lee, and J. Molburg, "Allocation of Energy Use in Petroleum Refineries to Petroleum Products: Implications for Life-Cycle Energy Use and Emission Inventory of Petroleum Transporation Fuels," *Int. J. Life Cycle Assess.*, vol. 9, no. 1, pp. 34–44, 2003.

[21] V. Manente, B. Johansson, and W. Cannella, "Gasoline partially premixed combustion, the future of internal combustion engines?," *Int. J. Engine Res.*, vol. 12, no. 3, pp. 194–208, 2011, doi: 10.1177/1468087411402441.

[22] Y. Yang, J. Dec, N. Dronniou, and W. Cannella, "Boosted HCCI Combustion Using Low-Octane Gasoline with Fully Premixed and Partially Stratified Charges," *SAE Int. J. Engines*, vol. 5, pp. 1075–1088, 2012, doi: 10.4271/2012-01-1120.

[23] A. B. Dempsey, "Dual-Fuel Reactivity Controlled Compression Ignition (RCCI) with Alternative Fuels," *University of Wisconsin-Madison PhD Dissertation (Mechanical Engineering)*. 2013.

[24] A. A. Amsden, P. J. O'Rourke, and T. D. Butler, "KIVA-II - A computer program for chemically reactive flows with sprays," 1989.

[25] A. A. Amsden, "KIVA-3V: A block-structured KIVA program for engines with vertical or canted valves," 1997.

[26] A. A. Amsden, "KIVA-3V, Release 2, improvements to KIVA-3V," 1999.

[27] Y. Ra and R. D. Reitz, "A reduced chemical kinetic model for IC engine combustion simulations with primary reference fuels," *Combust. Flame*, vol. 155, pp. 713–738, 2008, doi: 10.1016/j.combustflame.2008.05.002.

[28] A. B. Dempsey, B.-L. Wang, R. D. Reitz, B. Petersen, D. Sahoo, and P. C. Miles, "Comparison of Quantitative In-Cylinder Equivalence Ratio Measurements with CFD Predictions for a Light Duty Low Temperature Combustion Diesel Engine," *SAE Int. J. Engines*, vol. 5, no. 2, pp. 162–184, 2012, doi: 10.4271/2012-01-0143.

[29] R. D. Reitz, "Princeton University Combustion Energy Frontier Research Center (CEFRC)," *Combustion Summer School Lecture Series: Reciprocating Engines*, 2014. http://www.princeton.edu/cefrc/combustion-summer-school/archived-programs/2014-session/lecture-notes/#comp000053b7bb230000004a2e6291.

[30] A. B. Dempsey, N. R. Walker, and R. Reitz, "Effect of Cetane Improvers on Gasoline, Ethanol, and Methanol Reactivity and the Implications for RCCI Combustion," *SAE Int. J. Fuels Lubr.*, vol. 6, no. 1, 2013.

[31] A. B. Dempsey, S. Curran, and R. D. Reitz, "Characterization of Reactivity Controlled Compression Ignition (RCCI) Using Premixed Gasoline and Direct-Injected Gasoline with a Cetane Improver on a Multi-Cylinder Engine," *SAE Int. J. Engines*, vol. 8, no. 2, 2015, doi: 10.4271/2015-01-0855.

[32] B. Boyer *et al.*, "A Methodology to Determine Engine Efficiency Goals and Baselines." https://www.uscar.org/commands/files_download.php?files_id=353.

[33] D. Sahoo, B. Petersen, and P. C. Miles, "Measurement of Equivalence Ratio in a Light-Duty Low Temperature Combustion Diesel Engine by Planar Laser Induced Fluorescence of a Fuel Tracer," *SAE Int. J. Engines*, vol. 4, no. 2, pp. 2312–2325, 2011, doi: 10.4271/2011-24-0064.

[34] N. G. K. Raju, A. Dempsey, and S. Curran, "Analysis of

engine air handling systems for light-duty compression ignition engines using 1-D cycle simulation: Achieving high dilution levels for advanced combustion," in *ASME 2016 Internal Combustion Engine Fall Technical Conference, ICEF 2016*, 2016, doi: 10.1115/ICEF20169459.

[35] H. Solaka, U. Aronsson, M. Tuner, and B. Johansson, "Investigation of Partially Premixed Combustion Characteristics in Low Load Range with Regards to Fuel Octane Number in a Light-Duty Diesel Engine," *SAE Technical Paper 2012-01-0684*. 2012, doi: 10.4271/2012-01-0684.

[36] A. M. Ickes, S. V Bohac, and D. N. Assanis, "Effect of 2-Ethylhexyl Nitrate Cetane Improver on NOx Emissions from Premixed Low-Temperature Diesel Combustion," *Energy Fuels*, vol. 23, no. 10, pp. 4943–4948, 2009, doi: 10.1021/ef900408e.

[37] C. Noehre, M. Andersson, B. Johansson, and A. Hultqvist, "Characterization of Partially Premixed Combustion," *SAE Technical Paper 2006-01-3412*. 2006, doi: 10.4271/2006-01-3412.

[38] K. Akihama, Y. Takatori, K. Inagaki, and A. M. Dean, "Mechanism of the Smokeless Rich Diesel Combustion by Reducing Temperature," *SAE Tech. Pap. 2001-01-0655*, 2001, doi: 10.4271/2001-01-0655.

[39] J. Paz, D. Staaden, and S. Kokjohn, "Gasoline Compression Ignition Operation of a Heavy-Duty Engine at High Load," in *WCX World Congress Experience*, Apr. 2018, doi: https://doi.org/10.4271/2018-01-0898.

[40] T. Tsurushima, E. Kunishima, Y. Asaumi, Y. Aoyagi, and Y. Enomoto, "The Effect of Knock on Heat Loss in Homogeneous Charge Compression Ignition Engines," in *SAE Technical Paper 2002-01-0108*, 2002, doi: 10.4271/2002-01-0108.